Multinucleon Transfer Reactions: Recent Insights from Experiments at LNL-INFN

Tea Mijatović[1,*], *Suzana* Szilner[1], *Lorenzo* Corradi[2], *Franco* Galtarossa[3], *Petra* Čolović[1], *Josipa* Diklić[1], *Enrico* Fioretto[2], *Alain* Goasduff[2], *Giovanna* Montagnoli[3], *Alberto M.* Stefanini[2], *Jose Javier* Valiente Dobón[2], and *Giovanni* Pollarolo[4]

[1]Ruđer Bošković Institute, Zagreb, Croatia
[2]Istituto Nazionale di Fisica Nucleare - Laboratori Nazionali di Legnaro, Legnaro, Italy
[3]Dipartimento di Fisica, Universita di Padova, and Istituto Nazionale di Fisica Nucleare, Padova, Italy
[4]Dipartimento di Fisica, Universita di Torino, and Istituto Nazionale di Fisica Nucleare, Torino, Italy

Abstract. Transfer reactions are fundamental in nuclear structure and reaction mechanism studies. In heavy-ion transfer reactions, multiple nucleons can be transferred in a single collision, along with significant energy and angular momentum from the relative motion to the intrinsic degrees of freedom. Such multinucleon transfer reactions are essential for investigating a wide range of topics. This paper provides an overview of recent experiments performed using the PRISMA large solid-angle magnetic spectrometer. These experiments focused on studying nucleon-nucleon correlations with heavy-ion beams on medium-mass targets, as well as on the production mechanism of neutron-rich nuclei. The studies highlight the potential of transfer reactions for producing exotic species, particularly heavy neutron-rich nuclei.

1 Introduction

Transfer reactions play a crucial role in studying nuclear structure and reaction mechanism [1]. It is well established that, in the quasi-elastic regime, the mass and charge distributions of transfer products are governed by optimum Q-value considerations and transfer form factors [2]. For nuclei near the stability line, these considerations favor neutron pick-up and proton stripping channels, meaning that the lighter reaction fragment is likely to gain neutrons or lose protons. This makes multinucleon transfer reactions a valuable tool for producing neutron-rich nuclei associated with the lighter reaction partner.

As the neutron excess increases within the projectile, a shift in the transfer flux distribution is predicted, leading to a dominance of proton pick-up and neutron stripping channels for the lighter reaction partner [3, 4]. This transition from favoring neutron-poor to neutron-rich heavy products has been experimentally observed in various studies [5–7], highlighting the potential of multinucleon transfer reactions as an efficient mechanism for producing heavy neutron-rich nuclei, that are difficult to reach with other methods, such as fusion evaporation reactions and possibly with higher cross section than with the fragmentation reactions [6].

Our research aims to explore the most efficient pathways to produce these heavy neutron-rich nuclei, which has been a major focus of both theoretical and experimental studies in recent years. Specifically, we have concentrated on proton pick-up and neutron stripping for the lighter reaction partner, and neutron transfer channels for heavier systems. Additionally, understanding the impact of nucleon-nucleon correlations on transfer channel cross sections is a critical aspect of this work. To this end, we performed experiments in inverse kinematics at energies significantly below the Coulomb barrier, where quasi-elastic processes dominate, allowing for a detailed study of one- and two-nucleon transfer channels. These studies were made possible by employing the large solid-angle magnetic spectrometer PRISMA [8, 9], which offers high efficiency in identifying transfer products by mass, charge, and Q-value.

2 From quasi-elastic to deep-inelastic processes: the ^{206}Pb+^{118}Sn case

Multinucleon transfer (MNT) reactions between heavy ions at energies close to the Coulomb barrier constitute a link between quasi-elastic (QE) processes, characterized by the transfer of few nucleons and small kinetic-energy losses, and deep-inelastic collision (DIC) processes, where substantial nucleon transfer and large kinetic energy losses occur. The evolution from QE regime to DIC is particularly interesting for heavy-ion systems due to the pronounced influence of strong Coulomb fields and significant energy loss, which can greatly affect the final yield distributions. In the case of the ^{206}Pb+^{118}Sn system [10, 11], the optimal Q-values are well-suited for observing both neutron and proton pick-up and stripping channels, referring to changes in the lighter reaction partner. Specifically, the ground-to-ground state Q values for the main open channels lie below the bell-shaped curves

*e-mail: tea.mijatovic@irb.hr

that define the optimum Q values and, consequently, the transition probability.

In this study, we examined how, for such heavy system, the mass, charge yields and final cross sections depend on energy losses as the reaction evolves from the QE to the DIC regime. The goal is to provide a unified framework for understanding neutron and proton transfer channels in both pick-up and stripping directions.

We accelerated a ^{206}Pb beam to an energy of 1200 MeV onto a thin ^{118}Sn target. Target-like fragments were detected using the PRISMA spectrometer, positioned at a laboratory angle of 35° (grazing angle) and, for a short run, at 25°. This angular range was wide enough to observe the decrease in yield for elastic and inelastic scattering as well as the main region of multinucleon transfers. The use of inverse kinematics provided favorable experimental conditions, offering high resolution in mass (A), charge (Z), and Q-value due to the high kinetic energy (6-8 MeV/A) of the detected ions, and good efficiency due to the forward-focused angular distribution.

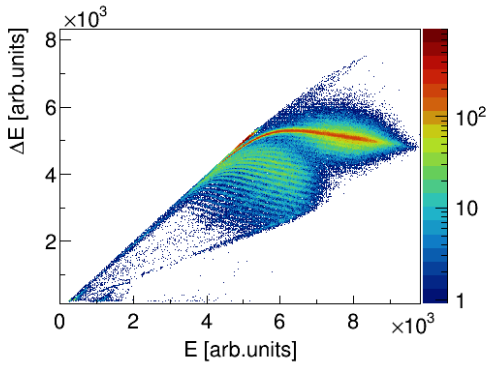

Figure 1. $\Delta E - E$ matrix obtained for the ^{206}Pb+^{118}Sn reaction at E_{lab}=1200 MeV, with the spectrometer placed at θ_{lab}=25°. The most intense band corresponds to the target-like nuclei. Figure taken from Ref. [10].

Figure 1 displays as an example the measured ΔE - E matrix. The most intense band corresponds to the target-like ions produced in the MNT reaction. We also observed some fission-like events, but only a fraction of their total yield because the spectrometer was optimized to detect transfer products. The visible Z separation indicates the good resolution of the ionization chamber.

The large acceptance of PRISMA provides an excellent opportunity to follow the energy dissipation in the reaction as it evolves from the QE to the DIC regimes. The best way to visualize this evolution is through Wilczynski plots, which map the Q-value (or, alternatively, kinetic energy) versus the scattering angle. We constructed these plots by selecting transfer reaction products in mass and charge, and generating Q-values under the assumption of a binary reaction and the momentum conservation. The Wilczynski plots are displayed in figure 2 for the strongest channels in the vicinity of the entrance-channel mass partition, specifically those involving the transfer of one and two neutrons, and one and two protons. At forward scattering angles, the distribution is dominated by a QE peak, located near the ground-to-ground state Q-value (Q_{gs}). This peak diminishes at angles more backward than the grazing angle where large energy-loss components become more prominent. For pure neutron transfers, the distributions peak near the Q_{gs} and extend to larger energy losses. Only in the elastic and inelastic channel, the narrow QE peak is well separated from the large energy-loss components. Channels involving proton and neutron stripping start near the optimum Q-values and peak at higher values, suggesting neutron evaporation. It is important to note that the overall effect of evaporation on the integrated yields of each neutron pick-up channel is much less significant, as higher-mass channels have progressively lower primary cross sections.

The total cross sections for various transfer channels are shown in figure 3, along with the GRAZING calculations [12, 13]. This model calculates how the total reaction cross section is distributed among the different reaction channels by treating QE and DIC processes on the same footing. GRAZING takes into account, besides the relative motion variables, the intrinsic degrees of freedom of projectile and target. These are the surface degrees of freedom and particle transfer. The exchange of many nucleons proceeds via a multi-step mechanism of single nucleons. Our results show good agreement between the GRAZING calculations and experimental data for pure neutron transfer channels and the pure (-1p) channel. However, on the proton-stripping side, the experimental cross sections shift towards lower masses and are increasingly underestimated by GRAZING. This discrepancy can partly be attributed to neutron evaporation from larger neighboring masses, significantly affecting the lower-mass region of populated isotopes. Similar discrepancies have been observed in previous studies involving medium-mass projectiles. Proton transfer channels tend to have larger energy losses, and differences between experimental and calculated cross sections were partly attributed to the large modification in the trajectories of entrance and exit channels due to the charge transfer, which may not be fully accounted for by theory. In the case of two-proton transfer channels, these discrepancies might also indicate the possible presence of additional degrees of freedom, such as pair-transfer modes. This progressive underestimation of yields as the number of transferred nucleons increases may indicate that more complex processes, not well taken into account by theory, populate the given isotopes. The observed different behaviour between the proton stripping and proton pick-up channels, which is especially relevant for the production of heavy neutron-rich nuclei, remains an open question for further investigation.

Further theoretical and experimental work is still required to better understand proton transfer channels, especially proton-pickup processes. This area has gained significant interest, particularly in developing new models that can predict cross sections using various approaches [4, 14, 15]. Therefore, the measured cross sections for the ^{206}Pb+^{118}Sn system have been compared with other theoretical models, including microscopic framework of time-dependent covariant density functional theory [15] and

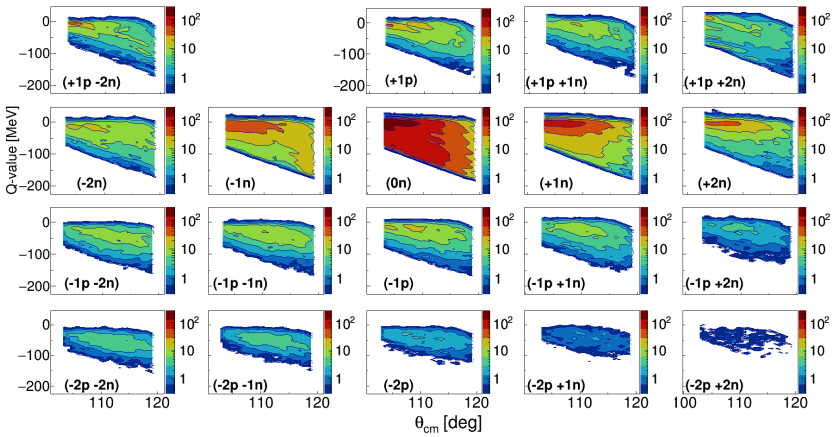

Figure 2. Wilczynski plots (Q-value vs $\theta_{\mathrm{c.m.}}$) measured at θ_{lab}=35° for the labeled transfer channels. The contours represent the double-differential cross sections, $d^2\sigma/d\Omega dQ$. The yield for the (+1p-1n) channel could not be safely extracted due to partial overlap with the ^{118}Sn one. Figure taken from Ref. [10].

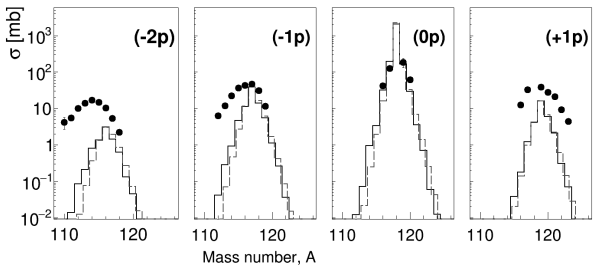

Figure 3. Experimental (points) and GRAZING calculated (histograms) total angle and Q-value integrated cross sections for the various transfer channels populated in the ^{206}Pb+^{118}Sn reaction at E_{lab}=1200 MeV. The solid and dashed histograms are the calculations performed with and without evaporation, respectively. Figure taken from Ref. [10].

theoretical framework that couples the Langevin dynamics iteratively with the master equation [16], demonstrating promising results in describing reaction dynamics.

3 Study of the heavy partner: the ^{197}Au+^{130}Te case

Primary yields in MNT reactions are often influenced by secondary processes, such as neutron evaporation, which typically shift mass distributions toward lower values. To investigate these mechanisms more thoroughly, a dedicated experiment was carried out using the ^{197}Au+^{130}Te system at energies near the Coulomb barrier [17]. This experiment focused on neutron transfer channels that lead to neutron-rich Au isotopes by using the neutron-rich ^{130}Te target. The PRISMA spectrometer was used in high-resolution kinematic coincidence with the NOSE time-of-flight system [18]. This setup allowed the coincident detection of both light and heavy transfer products: PRISMA identified isotopes in the tellurium region, while the coincident Au-like partners were detected with NOSE.

By using a high-resolution spectrometer in coincidence mode, a mass-mass correlation matrix was constructed, offering insights into the behavior of the heavy reaction partner. High-resolution identification of the light fragment's mass allowed the separation of the mass distribution of the heavy partner into well-defined bands. The centroids of bands when more neutrons are transferred were observed to shift slightly towards lower masses compared to the primary neutron transfer channels, indicating that primary fragments acquire significant excitation energy, leading to neutron evaporation. From this analysis, the average number of neutrons evaporated for each channel associated with Te isotopes was derived. The evaporation effect depends strongly on the bombarding energy and the projectile-target combination. Therefore, continuing these studies is essential to identify optimal conditions for using MNT reactions to populate heavy neutron-rich nuclei.

The experimental cross sections of Te isotopes, presented as points in figure 4, are compared with GRAZING calculations shown as histograms. The channels involving a few neutron transfers are quite well reproduced for both pick-up and stripping processes. However, the cross sections for the production of tellurium isotopes cannot be directly translated to those of the heavy reaction counterpart, as nuclear evaporation affects the light and heavy partners differently. Nevertheless, the agreement with the GRAZING calculations for the Te isotopes allows us to extend the predictions for the production of Au isotopes, shown in the bottom panel of the figure. Here, we also display the "production cross sections" to represent the evaporation effects as estimated by GRAZING. This comparison confirms that MNT reactions are indeed suitable method for producing neutron-rich heavy nuclei and highlights the importance of understanding secondary processes.

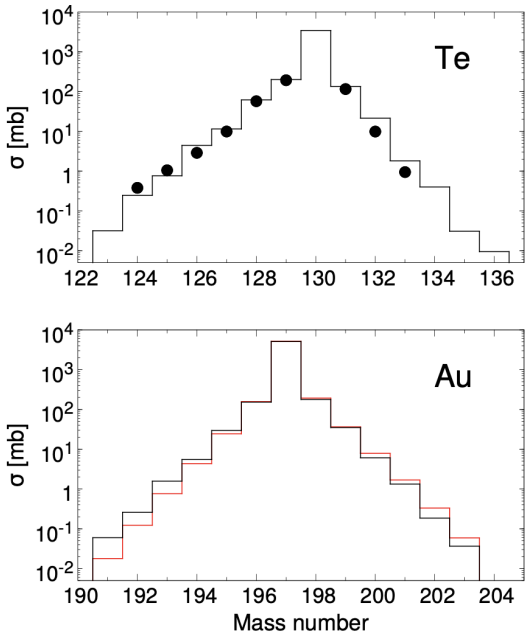

Figure 4. (Top) Total experimental cross sections of Te isotopes (points) and GRAZING calculations (histogram). (Bottom) GRAZING predictions for the Au isotopes with (black histogram) and without (red histogram) neutron evaporation. Figure taken from Ref. [17].

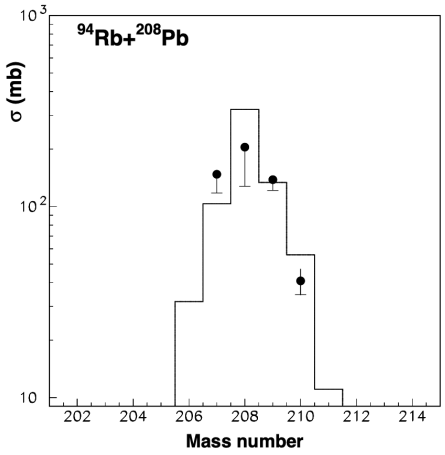

Figure 5. Total cross sections of Pb isotopes. The measured cross sections are indicated as lower limits, while those which include the estimated values for the ground states are indicated with full points. The histogram is the GRAZING prediction for E_{lab} = 575 MeV. Figure taken from Ref. [19].

4 Radioactive beams studies: the ^{94}Rb+^{208}Pb case

A recent experiment explored the potential of MNT reactions for producing neutron-rich heavy nuclei using neutron-rich beams in direct kinematics. A ^{94}Rb beam was accelerated to 6.2 MeV/nucleon, approximately 30% above the Coulomb barrier, and directed at a ^{208}Pb target [19]. Measurements were conducted at ISOLDE using the MINIBALL array [20] and the CD detector [21]. To allow a reliable comparison with theory, the focus was on pure neutron transfer channels, where modification in the trajectories of entrance and exit channels is minimal, and the nuclear form factors are better known.

The detector setup used enabled the identification of reaction products through their associated γ rays. For determining absolute cross-section values, the intensity of the lowest 3^- octupole state of ^{208}Pb at forward angles was used as a reference and was normalized to a distorted-wave Born approximation (DWBA) analysis. The cross sections for Pb isotopes are displayed in figure 5. The lower bars represent the directly measured γ yields, while the points include ground-state cross sections inferred from estimates. These values represent lower cross section limits, while the points also account for contributions from the Rb partner, assuming minimal mutual excitation. The GRAZING calculations, also shown in the figure, show good agreement with the experimental data, particularly for the neutron-rich Pb isotopes. In the higher mass region, the experimental cross section for ^{209}Pb is particularly well reproduced. The observed cross sections in the neutron-rich mass region confirm the predicted change in population pattern. This experiment is important for understanding the degrees of freedom which influence the evolution of the reaction and cross sections for the production of neutron-rich nuclei near the N=126 region, and is a first step towards comprehending this reaction mechanism's potential to access these hard-to-reach areas of the nuclear chart.

5 Study of proton transfer channels and the future perspectives with AGATA

Different degrees of freedom might be necessary to accurately describe the cross sections for the transfer of two nucleons, and it is interesting to investigate what happens at energies near and below the Coulomb barrier. Below the barrier, the reaction mechanism becomes simpler, resembling a more direct reaction. In these suitable conditions, two-nucleon transfer reactions can be used to investigate particle-particle correlations, induced by pairing interaction.

An advantage of heavy-ion transfer reactions is the ability to simultaneously compare observables for both single and pair transfer channels. However, in the proton sector, experimental data are very scarce, as proton transfer cross sections decrease more rapidly than those of neutrons, especially below the barrier. This makes proton transfer processes in heavy-ion collisions much less understood. They involve large modification in the trajectories of entrance and exit channels (due to the modification of the Coulomb field). Additionally, the single-particle level density for protons is less studied than the one of neutrons, and the corresponding single-particle form factors are less well known compared to neutrons. Proton transfer probabilities are also generally smaller at the same distances of closest approach.

Previous studies have been largely limited to above-barrier energies (to small values of distance of closest ap-

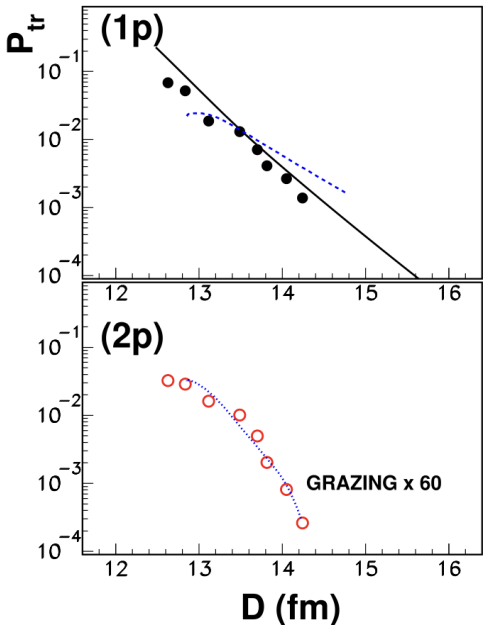

Figure 6. Transfer probabilities (P_{tr}) as a function of the distance of closest approach (D) for the pure proton stripping channels. Points are the experimental data: (1p) (full black circles), and (2p) (red empty circles). Solid lines are calculated transfer probability. (Top): The blue dashed line is the result of the GRAZING code calculation, while the full black line is the DWBA calculation. (Bottom): The blue dotted line corresponds to the GRAZING calculation for the (2p) channel, scaled × 60. Figure taken from Ref. [22].

proach, D), where overlapping with the absorption region complicates the interpretation of transfer probabilities and the extraction of enhancement factors. To address these challenges, the ^{116}Sn+^{60}Ni system was measured using the PRISMA spectrometer from above to well below the barrier, where secondary effects are minimized [22].

The data for proton stripping channels are represented as transfer probabilities, i.e., the ratio of transfer yield to quasi-elastic yield, plotted as a function of the distance of closest approach, which takes into account both beam energy and detection angle. Both experimental results and theoretical calculations are shown in figure 6. The results show that GRAZING calculations, which consider only independent nucleon transfer, significantly under-predict the experimental transfer probability for the 2p stripping channel by a factor of 60. This experiment is one of the few cases where proton transfer channels are measured below the barrier, minimizing the contributions from DIC and neutron evaporation. The analysis of total kinetic energy loss (TKEL) distributions indicates that energy dissipation remains limited, particularly at sub-barrier energies, where TKEL values align well with theoretical predictions (see Ref. [22] for more details). These findings support the dominance of direct QE processes, suggesting that the observed large enhancement factor cannot be attributed to significant energy losses or secondary effects.

In this context, the experiment "Probing nucleon-nucleon correlations in the ^{48}Ca+^{208}Pb system below the

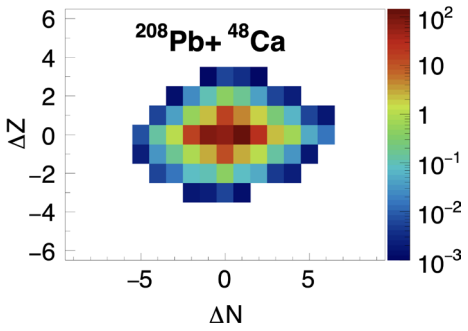

Figure 7. GRAZING calculated cross sections for the ^{208}Pb+^{48}Ca system at the beam energy of 1100 MeV. Relatively symmetric population of different stripping and pick-up channels is predicted.

Coulomb barrier" conducted in March 2023 with PRISMA coupled to AGATA holds significant importance [23]. Optimum Q-value considerations for this system indicate that the reaction populates not only the usual proton stripping and neutron pick-up (referred to the light partner) paths, but also the proton pick-up and neutron stripping ones, with comparable cross sections. This is clearly visible in figure 7 that shows the GRAZING calculated cross section for the target-like products in inverse kinematics. This opens very interesting opportunity to investigate correlations simultaneously for a complete set of transfer channels, involving both addition and removal of neutron and proton pairs. Additionally, we wanted to investigate whether any asymmetry exists between proton-stripping and proton-pickup channels. The employment of AGATA [24] will be crucial since it allows to study the transfer strength of different states, especially since the transfer for protons doesn't have to be dominated with the ground-to-ground state transitions.

6 Summary

The last generation of large solid-angle magnetic spectrometers, especially when combined with large γ-ray detector arrays, has significantly advanced MNT studies near the Coulomb barrier. Through the transfer of single and nucleon pairs, valuable insights into nucleon-nucleon correlations can be obtained, especially when experiments are conducted below the Coulomb barrier. Additionally, when many protons and neutrons are transferred, moderately neutron-rich nuclei that are difficult to access through other methods can be reached. This capability not only sheds light on yield distribution patterns, which are critical for understanding the underlying reaction mechanisms, but also facilitates detailed gamma spectroscopy giving insight to nuclear structure. A current area of interest is the investigation of the properties of the heavy neutron-rich binary partners in the reaction, which are important for both nuclear structure studies and astrophysics. However, secondary processes such as nucleon evaporation and transfer-induced fission may affect final yields, especially in heavier systems, requiring further investigation to opti-

mize MNT as a method for producing heavy neutron-rich nuclei.

Acknowledgments

This work was partly supported by the ENSAR2 Grant Agreement nb. 654002, and by the Croatian Science Foundation project no. IP-2018-01-1257, and in part by the Center of Excellence for Advanced Materials and Sensing Devices (Grant No. KK.01.1.1.01.0001). The material presented in this contribution is the result of the cooperative work of many people from different institutions and laboratories. We are particularly thankful to the gamma spectroscopy group of LNL and the AGATA and MINIBALL collaborations.

References

[1] R. M. Perez-Vidal, F. Galtarossa, T. Mijatović, S. Szilner, I. Zanon, D. Brugnara, J. Pellumaj, M. Ciemala, J. J. Valiente-Dobon, L. Corradi, E. Clement, S. Leoni, B. Fornal, M. Siciliano, A. Gadea, Nuclear structure advancements with multi-nucleon transfer reactions. Eur. Phys. J. A **59**, 114 (2023). https://doi.org/10.1140/epja/s10050-023-01027-2

[2] L. Corradi, G. Pollarolo, and S. Szilner, Multinucleon transfer processes in heavy-ion reactions. J. of Phys. G: Nucl. Part. Phys. **36**, 113101 (2009). https://doi:10.1088/0954-3899/36/11/113101

[3] C. H. Dasso, G. Pollarolo, and A. Winther, Systematics of isotope production with radioactive beams. Phys. Rev. Lett. **73**, 1907 (1994). https://doi:10.1103/PhysRevLett.73.1907

[4] V. Zagrebaev, and W. Greiner, Production of new heavy isotopes in low-energy multinucleon transfer reactions. Phys. Rev. Lett. **101**, 122701 (2008). https://doi.org/10.1103/PhysRevLett.101.122701

[5] T. Mijatović, Multinucleon transfer reactions: a mini-review of recent advances. Front. Phys. **10**, 965198 (2022). https://doi.org/10.3389/fphy.2022.965198

[6] Y. X. Watanabe *et al.*, Pathway for the Production of Neutron-Rich Isotopes around the N = 126 Shell Closure. Phys. Rev. Lett. **115**, 172503 (2015). https://doi.org/10.1103/PhysRevLett.115.172503

[7] T. Mijatović *et al.*, Multinucleon transfer reactions in the ^{40}Ar+^{208}Pb system. Phys. Rev. C **94**, 064616 (2016). https://doi.org/10.1103/PhysRevC.94.064616

[8] S. Szilner et al., Multinucleon transfer reactions in closed-shell nuclei. Phys. Rev. C **76**, 024604 (2007). https://doi.org/10.1103/PhysRevC.76.024604

[9] L. Corradi et al., Multinucleon transfer reactions: Present status and perspectives. Nucl. Instr. Meth. Phys. Res. B **317**, 743 (2013). https://doi.org/10.1016/j.nimb.2013.04.093

[10] J. Diklić *et al.*, Transfer reactions in ^{206}Pb+^{118}Sn: From quasielastic to deep-inelastic processes. Phys. Rev. C **107**, 014619 (2023). https://doi.org/10.1103/PhysRevC.107.014619

[11] S. Szilner *et al.*, Quest for Cooper pair transfer in heavy-ion reactions: The ^{206}Pb+^{118}Sn case. Phys. Rev. Lett. **133**, 202501 (2024). https://doi.org/10.1103/PhysRevLett.133.202501

[12] A. Winther, Grazing reactions in collisions between heavy nuclei. Nucl. Phys. A **572**, 191 (1994). https://doi.org/10.1016/0375-9474(94)90430-8

[13] A. Winther, Dissipation, polarization and fluctuation in grazing heavy-ion collisions and the boundary to the chaotic regime. Nucl. Phys. A **594**, 203 (1995). https://doi.org/10.1016/0375-9474(95)00374-A

[14] K. Sekizawa, TDHF theory and its extensions for the multinucleon transfer reaction: A mini review. Front. Phys. **7**, 20 (2019). https://doi.org/10.3389/fphy.2019.00020

[15] D. D. Zhang, D. Vretenar, T. Nikšić, P. W. Zhao, and J. Meng, Multinucleon transfer with time-dependent covariant density functional theory. Phys. Rev. C **109**, 024616 (2024). https://doi.org/10.1103/PhysRevC.109.024614

[16] F.C. Dai *et al.*, Theoretical study of multinucleon transfer reactions by coupling the Langevin dynamics iteratively with the master equation. Phys. Rev. C **109**, 024617 (2024). https://doi.org/10.1103/PhysRevC.109.024617

[17] F. Galtarossa *et al.*, Mass correlation between light and heavy reaction products in multinucleon transfer ^{197}Au+^{130}Te collisions. Phys. Rev. C **97**, 054606 (2018). https://doi.org/10.1103/PhysRevC.97.054606

[18] E. Fioretto *et al.*, A gas detection system for fragment identification in low-energy heavy-ion collisions. Nucl. Instr. Meth. Phys. Res. A A **899**, 73-79 (2018). https://doi.org/10.1016/j.nima.2018.05.011

[19] P. Čolović *et al.*, Population of lead isotopes in binary reactions using a Rb-94 radioactive beam. Phys. Rev. C **102**, 054609 (2020). https://doi.org/10.1103/PhysRevC.102.054609

[20] N. Warr et al., The Miniball spectrometer. Eur. Phys. J. A **49**, 40 (2013). https://doi.org/10.1140/epja/i2013-13040-9

[21] A.N. Ostrowski et al., CD: A double sided silicon strip detector for radioactive nuclear beam experiments. Nucl. Instr. Meth. Phys. Res. A **480**, 448 (2002). https://doi.org/10.1016/S0168-9002(01)00954-8

[22] L. Corradi *et al.*, Evidence of proton-proton correlations in the ^{116}Sn+^{60}Ni transfer reactions. Phys. Lett. B **834**, 137477 (2022). https://doi.org/10.1016/j.physletb.2022.137477

[23] T. Mijatović, L. Corradi *et al.*, LNL PAC Proposal, 2023.

[24] J.J. Valiente-Dobòn, *et al*. Conceptual design of the AGATA 2π array at LNL. Nucl. Instr. Meth. Phys. Res. A **1049**, 168040 (2023). https://doi.org/10.1016/j.nima.2023.168040